Research Article

Propellants, Explosives, Pyrotechnics

doi.org/10.1002/prep.202100191

Identification of the Degradation Products from α-Ionone Used as Stabiliser in "Green" Propellants through its Lifetime

Caroline Damseaux,*[a] Georges Scholl,[a] Christian Damblon,[b] Alain Dejeaifve,[c] Rowan Dobson,[c] Xiaofeng Ma,[d] Istvan Marko,[d] Jean-Christophe M. Monbaliu,[e] Edwin De Pauw,[a] and Gauthier Eppe[a]

Abstract: A stabiliser is added to gun and rocket propellants to react with species responsible for degradation during decomposition. Propellant powder manufacturers and army personnel are confronted with toxicity during powder degradation and must replace current stabilisers with non-toxic molecules. According to the STANAG 4582 (North Atlantic Treaty Organization (NATO) Standardisation Agreement [1]), propellant powders must remain chemically stable for a minimum of ten years when stored at temperatures equivalent to an isothermal storage (25 °C). Single and double base smokeless powders with α-ionone as a "green" stabiliser are tested and the results show that the heat flow is stable over time and that the autocatalysis occurs 2 to 3 times later than in powders with conventional stabilisers. This stabiliser is efficient for all nitrate ester-based propellants. In the present paper, we identify and monitor the evolution of the main degradation products over time by nuclear magnetic resonance (NMR), mass spectrometry (MS) to unravel the stabilisation mechanism under accelerated aging conditions. A time-related fluctuation of their respective amounts (increasing then decreasing, then re-increasing, …) is observed, which indicates that the daughter products have also a stabilisation effect. The three major α-ionone daughter products are identified as: 3-oxo-α-ionone, 4-oxo-β-ionone and 4,5-epoxy-α-ionone.

Keywords: α-ionone · Stabiliser · Propellant · Degradation · NMR

1 Introduction

An energetic material is a material containing a large amount of stored chemical energy that can be released in intense exothermic reactions when initiated by a stimulus. In weapon systems, energetic molecules are present in the same material as they are composed of an oxidiser and a fuel, both of which can be located in the same molecules. Nitrocellulose (NC) is often used in smokeless powder as an energetic material. The nitrate ester groups (R-ONO_2) confer the energetic character to these molecules. This function has a weak bond with the heteroatom, the nitro ester O–NO_2 bond that can be, for example, easily cleaved and carried out to homolytic degradation to form alkoxy and nitro radicals (Figure 1). Nitrate ester compounds are chemically unstable and degrade with time, heat, humidity and light. In most cases, propellant powders are composed of the energetic binder NC, which is produced by the nitration of cellulose in a mixture of nitric acid (HNO_3) and sulfuric acid (H_2SO_4). Its polymeric character gives the material flexibility and allows it to retain its original shape [2,3].

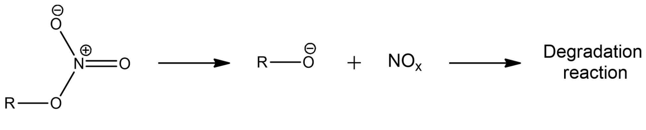

Figure 1. Homolytic decomposition of nitrate esters [2].

The presence of products such as alkoxy radicals (R–O.), nitrogen oxides (NO_x) and residual acids (HNO_3) accelerate powder degradation by attacking the yet undecomposed nitrate esters from NC in the propellant matrix. A succession

---

[a] C. Damseaux, G. Scholl, E. De Pauw, G. Eppe
Mass Spectrometry Laboratory, MolSys Research Unity, Université de Liège, 11, allée du six Août, 4000 Liège, Belgium
**e-mail: c.damseaux@uliege.be*

[b] C. Damblon
Structural biological chemistry laboratory, MolSys Research Unity, Université de Liège, 11, allée du six Août, 4000 Liège, Belgium

[c] A. Dejeaifve, R. Dobson
R and D department, PB Clermont (Eurenco), 176, rue de Clermont, 4480 Engis, Belgium

[d] X. Ma, I. Marko
Laboratory of Organic and Medicinal Chemistry, Université Catholique de Louvain, Place Louis Pasteur 1, 1348 Louvain-la-Neuve, Belgium.

[e] J.-C. M. Monbaliu
Center for Integrated Technology and Organic Synthesis, MolSys Research Unity, Université de Liège, 11, allée du six Août, 4000 Liège, Belgium

Supporting information for this article is available on the WWW under https://doi.org/10.1002/prep.202100191

of secondary reactions like acid-base reactions, hydrogen abstractions and oxidations occur and produce gases such as CO, and especially NO and NO_2 [2,4]. These reactions have been studied using calorimetric tests which have revealed a loss of energy and an increase in temperature of the powder, which influences the performance of the propellant and reduces its lifetime [5–10].

Stabilisers are added to propellants to prevent unfortunate events such as deflagration, exothermic reactions or auto-catalysis. Its purpose is to react with alkoxy and nitro radicals coming from homolyses of NC during its decomposition. Without a stabiliser, alkoxy and nitro radicals have a catalytic effect on the degradation rate. Stabilisers reduce the deterioration of the propellant by reacting with free radicals (R–O. and/ or NO_x) [4,6,11,12]. It avoids self-ignition and has a higher probability of occurring due to accelerated decomposition. It is mandatory to address these safety issues because these exothermic reactions have already caused incidents in the defence industry [4,13].

Conventional stabilisers for nitrocellulose-based propellants belong to two classes: aromatic amines and aromatic urea derivatives [14]. Three stabilisers are often added to the propellant to slow down the degradation process: diphenylamine (DPA), ethyl centralite (EC) and akardite II (Ak II).

The natural degradation of stabilisers produces toxic species during the propellant's lifetime, for example DPA and Ak II, which decompose to form the unstable intermediate N-nitroso-diphenylamine (N-NO-DPA) shown in Figure 2 [4,6,15,16]. The problems are similar for EC. There is a rapid presence of N-NO derivatives which are more carcinogenic because part of the amine is an alkyl.

In the past few years, new less harmful stabilisers have been studied such as triphenylamine (TPA) [17,18], malonanilide derivatives [19–23], activated aromatic ether [24] and zeolites [25]. Most of these molecules are too rapidly consumed in the powders, which challenges their stabilisation capabilities.

It is therefore necessary to study and develop new generations of stabilisers that have the main properties of being slowly consumed and that are even not toxic. This last criterion is essential in the light of the current REACh regulation, which requires that old stabilisers be replaced by "greener" products [14,26–28]. Dejeaifve et al. demonstrate that stabiliser such as 2,3,5-trimethylphenol, 1,2,3-trimethoxybenzene, α-ionone, curcumin and α-tocopherol are able to stabiliser nitrate esters [2,26,29]. These stabilisers are efficient for all nitrate ester-based propellants, and so mainly gun propellants, however also rocket propellants containing nitrocellulose.

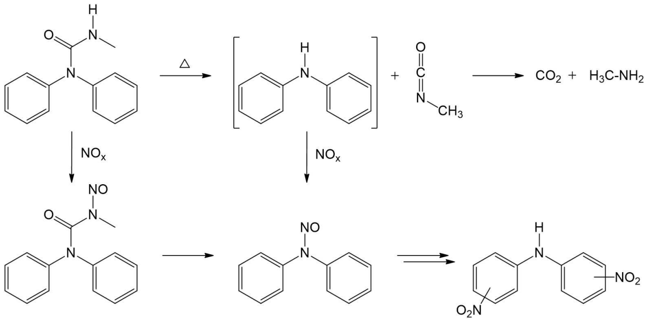

Figure 2. Carcinogenic N-nitrosamines produced by Ak II [2].

Double base powders with α-ionone are tested and it is shown that the heat flow is stable over time and that autocatalysis occurred 1.5–4 times later than powders with DPA, Ak II or EC as stabiliser [29,30]. A-ionone belong to the family of rose ketones and come from the degradation of β-carotene. It is well-known for participating in the scent of violets and in perfume compositions. It is an environmentally-friendly stabiliser, which does not produce any mutagenic or carcinogenic daughter products for stabilising a nitrate ester- based propellant. The degradation system of this stabiliser in the powder matrix has to be deeply understood to prove the potential of this greener molecule. For that purpose, the degradation products of the α-ionone have to be characterised first to explain this mechanism.

2 Experimental Section

2.1 Chemicals

For chromatographic separation, analytical grade (dichloromethane, DCM) and high pressure liquid chromatography (HPLC) grade solvents (methanol, acetonitrile (ACN) and water) are bought from Biosolve (Valkenswaard, the Netherlands). Single-use syringes (2 mL) with a luer tip are from VWR. Target2™ PTFE Syringe Filters, 0.45 μm, 30 mm, with Pre-Filter, are purchased from Thermo Fisher Scientific (North-America). For NMR acquisitions, deuterated chloroform (99.96% + 0.03% tetramethylsilane (TMS)) is obtained from Eurisotop (Saint-Aubin, France). The 90% pure technical-grade standard of α-ionone is purchased from Sigma-Aldrich (Overijse, Belgium). Eurenco (Engis, Belgium) produced the single and double base powder (at lab scale) with α-ionone as stabiliser. The composition of the propellants are as follow for single base (stabiliser ≈1%, graphite ≈0.2%, NC: remainder) and for double base (nitroglycerine (NG) ≈10%, deterrent ≈5%, stabiliser ≈1%, graphite ≈0.2%, NC: remainder [2]).

Most of the commercial powders are double bases but, in order to reduce matrix effects and manipulation risks, we used single base powder as model. The ageing was extended up to 10 days at 90 °C to comply with the STANAG 4582 protocol.

2.2 HPLC Conditions

The separations are performed on an Agilent 1100 series HPLC system (Agilent Technologies, Palo Alto, USA) equipped with a diode array detector (DAD). Acquisition and data treatment are carried out with ChemStation. Two columns are used. The first is a reversed phase ZORBAX SB–C18 column (Agilent Technologies, Palo Alto, USA), 4.6×150 mm and 5 μm particle size used for the analytical part. The second is a semi-preparative ZORBAX SB–C18 column (Agilent Technologies, Palo Alto, USA), 9.4×150 mm and 5 μm particle size, are employed to collect enough sample for NMR acquisitions. A ZORBAX SB–C18, 4.6×5 mm with 1.8 μm, ultra high pressure liquid chromatography (UHPLC) guard column is installed to protect the analytical columns.

A water : ACN gradient mix is used as mobile phase as follows: 30% of ACN for 9 min, increased by 10% until 90% every 10 minutes for a total runtime of 69 minutes. The autosampler and the column are kept at RT. The detection frequency is set at a wavelength of 228 nm. The injection volume and the flow rate are dependent on the inner diameter of the column: for the classical ZORBAX SB–C18 it is 30 μL and 0.6 mL/min, and for the semi-preparative ZORBAX SB–C18 100μL and 2.4 mL/min.

2.3 NMR Conditions

Spectra are acquired using a Bruker Ultrashield Plus 700 MHz equipped with a helium cold probe (cryoprobe) (Bruker, BioSpin GmbH, Germany).

In order to identify all the protons in each molecule, proton spectra (^{1}H) are acquired with 64 scans and with a spectral width of 14097.7 Hz. Chemical shifts are referenced to TMS.

Heteronuclear single quantum coherence spectra (^{1}H-^{13}C HSQC) are acquired with eight scans and the data are collected with a spectral width of 11160.7 Hz in the ^{1}H (F2) dimension, and 29051.7 Hz in the ^{13}C (F1) dimension with time domain (TD) of 256 K for channel F1.

Heteronuclear multiple bond coherence-nuclear spectra (^{1}H-^{13}C HMBC) are acquired with 16 scans and the data are collected with a spectral width of 6756.8 Hz in the ^{1}H (F2) dimension, and 38736.6 Hz in the ^{13}C (F1) dimension with TD of 256 K for channel F1.

Double quantum filtered correlation spectroscopy spectra (^{1}H-^{1}H DQF-COSY) are acquired with four scans and the data are collected with a spectral width between 6756.8 to 9090.9 in both dimensions with TD of 128 K for channel F1.

Total correlation spectroscopy spectra (TOCSY) are acquired with eight scans and the data are collected with a spectral width between 6756.8 to 10504.2 in both dimensions with TD of 256 K for channel F1.

The NMR data are processed using Topspin 3.4.1 software (Bruker BioSpin GmbH, Germany).

2.4 Gas Chromatography – Mass Spectrometry (GC-MS) Conditions

To identify the daughter products, samples are analysed by two different mass spectrometers: the first is a gas chromatography with an atmospheric pressure chemical ionization (APCI) source and a high-resolution mass spectrometry time of flight coupled to trapped ion mobility (GC-APCI-timsTOF, Bruker), and the second is a unit mass resolution tandem mass spectrometry coupled to gas chromatography with and electron ionisation (EI) source (GC-EI-MS^n, Polaris-Q, Thermo). Injections are done on both instruments with the same GC parameters: separation on a RTX-5 ms, 30 m×0.25 mm×0.25 μm (Restek) GC column, with a 1 mL/min He (6.0 purity, Air Liquide) flow and an oven temperature program beginning at 40 °C for 2 min, ramped at 10 °C/min to 170 °C hold 1 min, then increased at 5 °C/min to 220 °C and finally to 310 °C at 10 °C/min kept 5 minutes.

Each source has its advantages. The APCI source allows an efficient ionisation of the substrate as it occurs at atmospheric pressure, and thus has a high collision frequency. This soft ionisation produces ions of the molecular species with few fragmentations in comparison with other methods. The EI source is a non-selective ionisation and provides fragmentation spectra with structural information and the fingerprint of compounds.

On the timsTOF, ions are produced with an APCI source set in positive mode with the following parameters: capillary voltage at 4500 V, Corona at 8000 nA, nebuliser pressure at 0.24 MPa, dry gas flow at 1.5 L/min and the drying temperature set at 175 °C). The acquisitions are made between 0.50 and 1.35 V.s/cm^2 in mobility and between 50 to 1000 m/z in full scan mode.

On the Polaris-Q, ions are produced with an EI source in positive mode set at 70 eV and 250 °C. The two most intense ions are then isolated and fragmented with 2 V energy and the full pattern of daughter ions are recorded (35 to 500 m/z).

2.5 Sample Preparation

The powder is aged for up to 10 days at 90 °C, in sealed, fully filled vials, to replicate these storage conditions over an even longer period in order to generate sufficient degradation species as the single base degrades much slower than the double base.

For MS, the extraction of α-ionone degradation products is as follows: addition of DCM (30 mL) to sample (1 g) stored in a dark place for 24 hours. The supernatant phase is deposited in a clean vial and is evaporated to dryness (40 °C) and under a nitrogen stream. The sample is reconstituted with methanol (1 mL) and then is filtered through a 0.45 μm PTFE filter syringe before analysis [31].

For NMR, a larger sample intake (5 g) of smokeless powder is required to perform NMR acquisitions.

3 Results and Discussion

3.1 Optimisation of the Extraction

Three methods are compared for the extraction of α-ionone. The first is developed by Wissinger and McCord and consists of purifying the powder with petroleum ether to remove naphthalene derivatives that interfere with the degradation products [31]. Subsequently, the analytes are extracted by several liquid-liquid extractions with DCM. Ideally, three petroleum ether washes and three DCM extractions are required.

The second method is published by Reese and consists of dissolving the propellant in acetone [32]. Once the powder is dissolved, compounds of interest are extracted with DCM. This method are discarded because there is formation of films of NC in the evaporation step avoiding the process to run smoothly and achieve good extraction yields

The third method is developed by Lopez-Lopez and consists of extracting α-ionone and its daughter products with methanol [33]. The extraction continues by adding DCM and then performing a third extraction with methanol to recover the set of the degradation compounds. This is only necessary in the case of double and triple base powders. As methanol is also a polar solvent, the same daughter products are recovered at the end of extraction as with the Wissinger method. However, DCM has a lower boiling point than methanol and therefore the experiment takes less time to complete.

In each of these methods, DCM is used to extract α-ionone and its daughter products. It appeared to be the most appropriate solvent. It has a good affinity to extract polar target compounds. The first method established by Wissinger is the most appropriate for this study. With these tests, we demonstrated that for a single base powder, the petroleum ether is not necessary because the retention times of naphthalene derivatives are greater than the degradation products of the α-ionone and the intensities are negligible.

3.2 Separation of Degradation Products by HPLC

Extracted molecules are separated by HPLC on a C18 column and detected by UV using the gradient described in Figure 3 highlights the separation of α-ionone and its

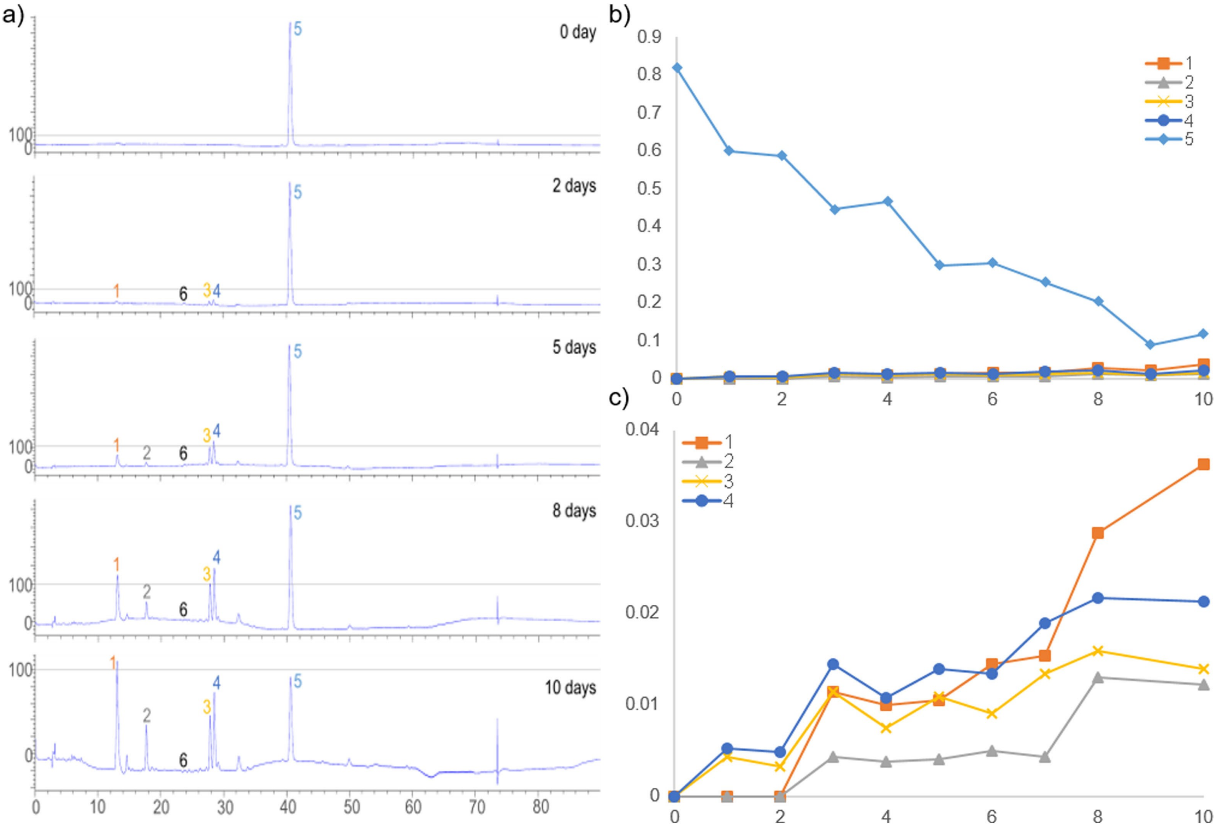

Figure 3. Evolution of α-ionone (5) and its degradation products (1, 2, 3, 4, 6) during thermal ageing; a) HPLC chromatogram after extractions on 1 g of single base powder with stabiliser and detected by ultraviolet (UV) at different steps of ageing, relative abundance on y-axis and minutes on x-axis; b) evolution of α-ionone and their daughter products (in percentage on y-axis) relative to powder ageing (in years on x-axis); c) zoom on Figure 3b.

daughter products over time. A retention time greater than three times the dead volume is achieved for the major compounds. An overlap is observed for compounds 3 and 4. We can see a step resolution of the α-ionone signal, which stabilise at 95% degradation rate after 10 days corresponding to 30 years (Figure 3a).

Figure 3 shows the decrease of α-ionone and the evolution of the four daughter products over time during thermal ageing. Analytes 3 and 4 appeared from the first day of ageing, which is equivalent to just under 3 years of natural ageing (according to STANAG 4582, concerning heat flow calorimetry). Compounds 1 and 2 appeared from the third day, or just before 9 years of natural ageing.

Figure 3b shows that the daughter product signals increase in a stepwise pattern during the ageing process. These fluctuations are due to a stabilising role of the propellant powder played by daughter products. We have therefore observed that their quantity changes over time because they are produced and consumed simultaneously over time. During ageing, the stabiliser and its daughter products are consumed.

3.3 Identification of Degradation Products by NMR and MS

The four selected predominant compounds detected by HPLC-UV are collected and identified by NMR and MS.

The combined information from these two techniques are complementary to identify the functions and their positions. The aim is to obtain complementary information on the structure of the molecules; the fragments have provided additional data to verify identification of daughter products [34]. The syntheses of degradation products were also performed to confirm the identified products (see supplementary data).

In each NMR spectrum, traces of NC coming from the propellant that could not be completely removed during the extraction steps gave a parasite signal. They are observed in two different regions of the chemical shift (δ): 1.20 ppm < δ < 1.47 ppm and 2.01 ppm < δ < 2.08 ppm (grey discontinuous lines on Figure 4 and Figure 5).

3.3.1 Degradation Product 1

The first compound eluted from the HPLC column at 13.1 min (number 1 on the Figure 3) is collected for analysis.

Initially, it is characterised by GC-APCI-timsTOF to identify the molecular mass. The singly charged molecular ion with a ratio of m/z = 207.13 (M + H) provided information on the molecular weight of the identified compound ($C_{13}H_{18}O_2$). The fragmentation spectrum, with Polaris-Q Ion Trap, has given further insights into the structure of the first degradation product with a base peak at m/z = 108 (M^+, 100%).

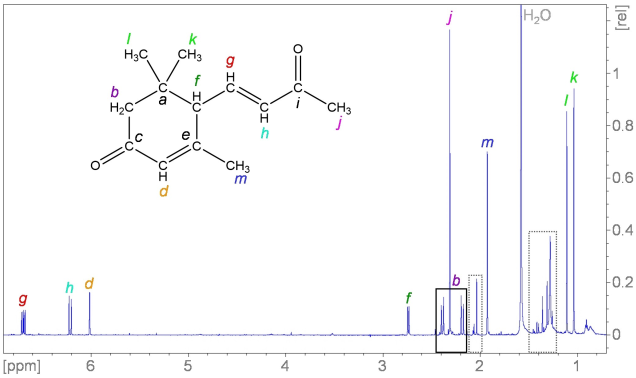

Figure 4. ^1H NMR spectrum of 3-oxo-α-ionone obtained at 700 MHz, showing ten resolved proton lines that can be assigned to the different proton sites of the structure.

NMR is subsequently used to determine the molecular structure. The following peaks can be observed in Figure 4, showing the ^1H NMR spectrum (700 MHz, $CDCl_3$, 25 °C) δ = 6.69 (dd, J = 9.6 Hz, J = 15.8 Hz, 1H), 6.21 (d, J = 15.8 Hz, 1H), 6.01 (s, 1H), 2.73 (d, J = 9.6 Hz, 1H), 2.39 and 2.18 (dd, J = 16.9 Hz, 2H), 2.31 (s, 3H), 1.92 (s, 3H), 1.11 (s, 3H), 1.03 (s, 3H).

The ^{13}C NMR spectrum (700 MHz, $CDCl_3$, 25 °C) provide δ = 198.2, 197.5, 159.1, 143.7, 133.9, 127.0, 55.6, 47.5, 28.0, 27.7, 27.5, 23.6 ppm.

The HSQC spectrum stated that the protons with the following chemical shifts (number 2, δ = 2.39 ppm and 2.18 ppm) are found in non-equivalent environments, even if they belong to the same carbon atom (δ = 46.34 ppm; Figure 4). This indicated that it is a CH_2 function on the cycle. The HMBC spectrum suggested the presence of a second carbonyl bond (δ = 198.26 ppm) on the ring. The carbon of the carbonyl function is coupled with the two non-equivalent protons (number 2, δ = 2.39 ppm and 2.18 ppm). The COSY and TOCSY spectra have confirmed the connections between the protons in the molecule and the neighbouring groups.

With these data, we identified the ketone form of α-ionone, which is named 3-oxo-α-ionone (Figure 4).

3.3.2 Degradation Product 2

The second compound getting out of the HPLC column at 17.7 min is collected for analysis. Like the first degradation product, the same monocharged molecular ion is observed but the fragmentation spectrum is distinct with a base peak at m/z = 163 (M^+, 100%).

Next, it is characterised by NMR to determine the molecular structure. The following peaks are observed in the ^1H NMR spectrum in Figure 5 (700 MHz, $CDCl_3$, 25 °C) δ = 7.24

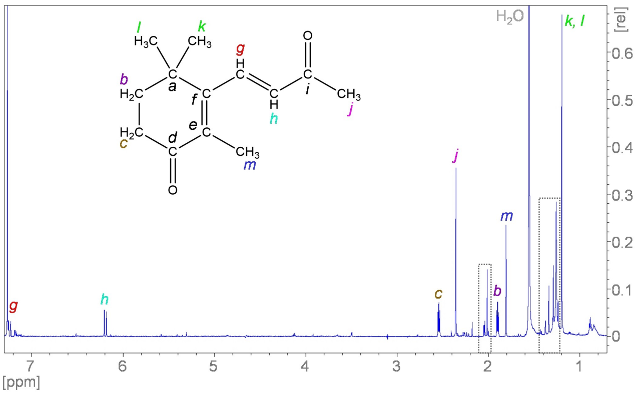

Figure 5. ^{1}H NMR spectrum of 4-oxo-β-ionone obtained at 700 MHz. The one-dimensional spectrum shows seven resolved proton lines that can be ascribed to the different proton sites of the structure.

(d, J = 16.5 Hz, 1H), 6.19 (d, J = 16.5 Hz, 1H), 2.54 (t, J = 6.9 Hz, 2H), 2.35 (s, 3H), 1.89 (t, J = 6.9 Hz, 2H), 1.80 (s, 3H), 1.19 (s, 6H).

The ^{13}C NMR spectrum (700 MHz, $CDCl_3$, 25 °C) provide δ = 198.6, 197.4, 157.8, 140.4, 133.5, 131.4, 37.3, 34.2, 27.9, 27.3, 13.4, 13.4 ppm.

The HSQC spectrum assigned all protons and carbons together and revealed that the double bond is no longer at the same position on the cycle (Figure 5). It is a molecule derived from the β-ionone form. The HMBC spectrum indicated the presence of a second carbonyl bond (δ = 198.59 ppm) which is on the ring. The carbon of the carbonyl function is coupled with the four protons of CH_2 groups (red and purple, δ = 2.54 ppm and 1.89 ppm) and with the three protons of CH_3 groups (blue, δ = 1.80 ppm) carried by the quaternary carbon. The COSY and TOCSY spectra have confirmed the connections between the protons in the molecule and the neighbouring groups.

With this information, we are able to identify the ketone form of β-ionone, which is named 4-oxo-β-ionone (Figure 5).

3.3.3 Degradation Product 6

The compounds 3 and 4 on the Figure 3 are analysed and identified as a mixture of several isomers. Unfortunately, the lack of separation did not allow us to clearly identify the structure of individual isomers, only common patterns are available.

The third degradation product (rt 23.8 min – compound 6 in Figure 3) is present in small quantities in the simple base powder, it is in the background noise. However, it found in higher quantities in double base powder than in single base, therefore it is identified after extraction from the double base powder. GC-APCI-timsTOF revealed a protonated single charged molecular ion at m/z = 209.15 which correspond to the molecular formula $C_{13}H_{20}O_2$. But for the same retention time in GC, several peaks of mobility are observed ($1/K_0$ = 0.612, 0.910, 0.978 and 1.319 V s/cm^2). Similarly, a unit resolution full scan mass spectrum in EI+ showed that there is a perfect coelution (in either GC or LC) with a second compound of lower mass. Deconvolution of the full scan mass spectra in combination with the information from the other techniques allowed us to identify the possible structure of the daughter product as 4-(1,3,3-trimethyl-7-oxabicyclo[4.1.0]hept-2-yl)-3-buten-2-one. To prove the identification, those results are compared to the analysis of the commercial 4-(1,3,3-trimethyl-7-oxabicyclo[4.1.0]hept-2-yl)-3-buten-2-one. With the same retention times in LC and GC, the same molecular ions and the same fragmentation pattern in EI+ mass spectrometry (Figure 6), there is enough evidence to conclude that the third daughter product is 4-(1,3,3-trimethyl-7-oxabicyclo[4.1.0]hept-2-yl)-3-buten-2-one also named 4,5-epoxy-α-ionone.

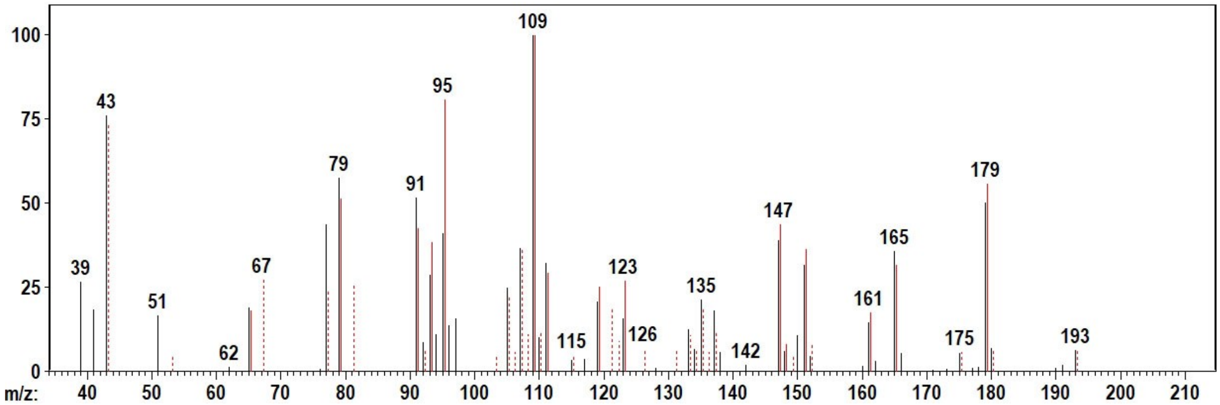

Figure 6. Extracted spectrum (red continuous lines) and uncertain peaks (red discontinuous lines) of compound 6 by comparison with the standard of 4,5-epoxy-α-ionone (black lines) with Polaris-Q Ion Trap.

3.4 Proposed Degradation Mechanism

The identification of the products allows us to propose a degradation mechanism for α-ionone in a single base propellant powder. Formation of these degradation products occurred in a matrix that is highly oxidising and acidic [35].

The large portion of NC gives access to $-ONO_2$ groups that provide the oxidiser source and the propellant matrix provides a low pH medium needed for further reaction (Figure 7).

In a first step, a radical species arising from the decomposition of the NC (i.e. an alkoxy radical) abstracts the most labile hydrogen of the α-ionone, leading to the formation of a radical α-ionone (A) [36]. This intermediate has a high reactivity and cannot be isolated. Two oxidation pathways could subsequently take place, from recombination with either free oxygens or with a nitro species produced by the decomposition of the propellant [37]. In the first case, the peroxy-radical formed can, in turn, abstract a hydrogen from the NC matrix, affording the compound (C) that could in an intermolecular reaction yield the epoxide 6 and the alcohol (D) [38]. This alcohol could in turn be oxidised into the ketone form (1). Another explanation for the formation of the ketone could come from the homolytic scission of the nitrogen-oxygen bond of molecule (F), formed by the oxidation of the nitrite intermediate [39]. Loss of the NO_2 cluster occurs to give a radical oxygen on the cycle. Eventually, this molecule can be either hydrolysed or oxidised to lead to the formation of the ketone form of α-ionone, 3-oxo-α-ionone, which is the first degradation product.

A similar mechanism can also transform the β-ionone (also present in the powder) into its ketone form, 4-oxo-β-ionone.

4 Conclusion

A-Ionone, used as stabiliser for all nitrate ester-based propellants, is slowly degraded into daughter products, which are themselves able to be further degraded. This chain degradation allows α-ionone to act as a stabiliser for over 10 years, as recommended by NATO. With a series of extractions, separations, NMR and MS analyses, we proved that the proposed theoretical degradation mechanism is true by identifying the three major daughter products:

- 3-oxo-α-ionone
- 4-oxo-β-ionone
- 4,5-epoxy-α-ionone

Their formation during the ageing process is due to the reaction mixture rich in oxygen and nitric acid. These degradation products are also stabilisers; their quantity varies over time as they are formed and consumed. A future study has to evaluate the toxicity of each daughter product from α-ionone in order for them to be accepted as stabilisers.

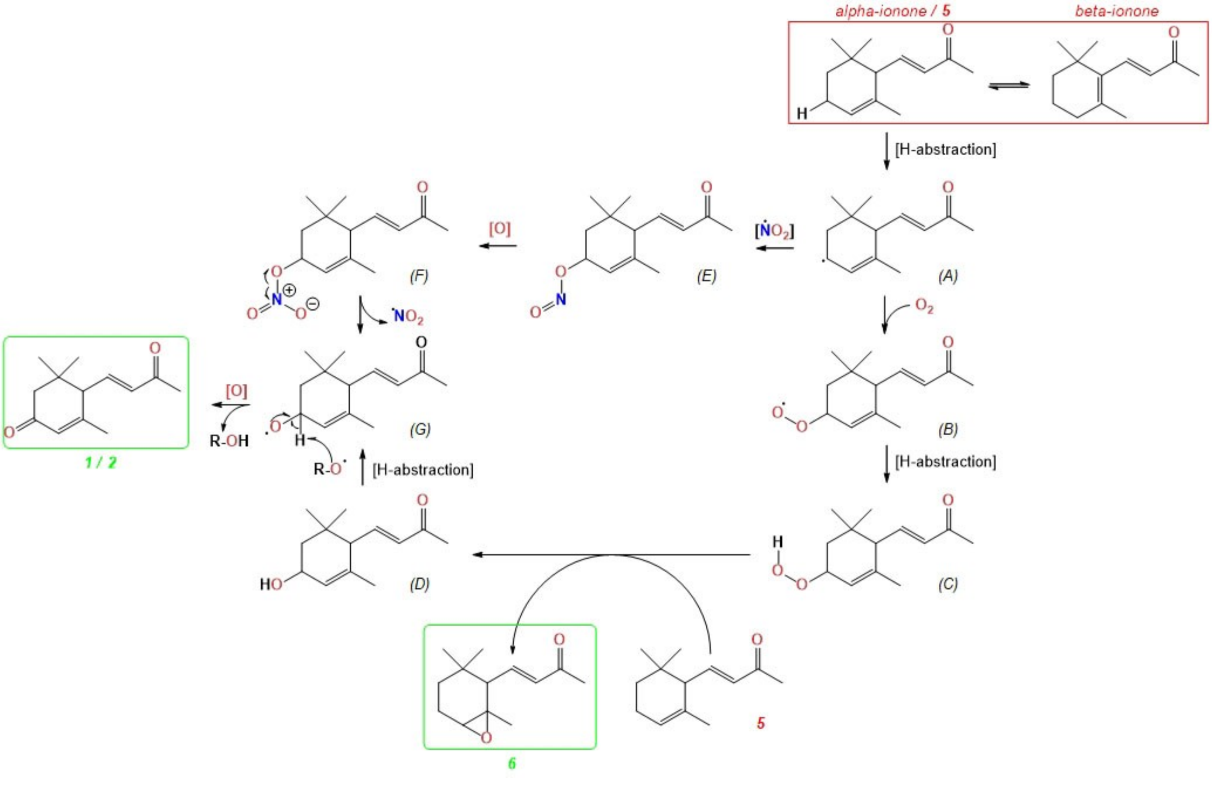

Figure 7. The proposed reaction mechanism of the α-ionone degradation into their daughter products (1, 2 and 6) [26].

Symbols and Abbreviations

ACN	Acetonitrile
Ak II	Akardite II
APCI	Atmospheric Pressure Chemical Ionisation
COSY	Correlation Spectroscopy
DCM	Dichloromethane
DPA	Diphenylamine
EC	Ethyl Centralite
EI	Electronic Impact
GC	Gas Chromatography
GC-APCI	Gas Chromatography – Atmospheric Pressure Chemical Ionisation
HMBC	Heteronuclear Multiple Bond Correlation
HPLC	High Pressure Liquid Chromatography
HSQC	Heteronuclear Single Quantum Coherence
LC	Liquid Chromatography
MS	Mass Spectrometry
NATO	North Atlantic Treaty Organization
NC	Nitrocellulose
NG	Nitroglycerine
NMR	Nuclear Magnetic Resonance
N-NO-DPA	N-nitroso-diphenylamine
PTFE	Polytetrafluoroethylene
TD	Time Domain
timsTOF	Trapped Ion Mobility Spectrometry – Time Of Flight
TMS	Tetramethylsilane
TOCSY	Total Correlation Spectroscopy
TOF	Time Of Flight
TPA	Triphenylamine
UHPLC	Ultra High Pressure Liquid Chromatography
UV	Ultraviolet

Acknowledgements

The authors are grateful to the MecaTech cluster for the subsidies granted under Convention No. 7841 on a technological innovation partnership entitled NextGeneration Powder, implemented by the Walloon competitiveness cluster in mechanical engineering.

Data Availability Statement

Data available on request due to privacy/ethical restrictions.

References

[1] NATO Standardization Agreement (NATO STANAG) 4582, Explosives, Nitrocellulose Based Propellants, Stability Test Procedure and Requirements Using Heat Flow Calorimetry, *NSA-(2007)0*, **2007**.

[2] A. Dejeaifve, A. Fantin, L. Monseur, R. Dobson, Making Progress Towards «Green» Propellants, *Propellants Explos. Pyrotech.* **2018** *43*, 831–837, DOI:10.1002/prep.201800026.

[3] E. Rozumov, Recent Advances in Gun Propellant Development: From Molecules to Materials, Springer Nature, **2017**, *25*, DOI:10.1007/978-3-319-59208-4_2.

[4] W. P. C. De Klerk, Assessment of Stability of Propellants and Safe Lifetimes, *Propellants Explos. Pyrotech.* **2015**, *40*, 388–393, DOI:10.1002/prep.201500040.

[5] T. B. Brill, P. E. Gongwer, Thermal Decomposition of Energetic Materials 69. Analysis of the Kinetics of Nitrocellulose at 50 °C-500 °C, *Propellants Explos. Pyrotech.* **1997**, *22*, 38–44, DOI:10.1002/prep.19970220109.

[6] K. Katoh, S. Yoshino, S. Kubota, Y. Wada, Y. Ogata, M. Nakahama, S. Kawaguchi, M. Arai, The Effects of Conventional Stabilizers and Phenol Compounds Used as Antioxidants on the Stabilization of Nitrocellulose, *Propellants Explos. Pyrotech.* **2007**, *32*, 314–321, DOI:10.1002/prep.200700034.

[7] P. Guillaume, M. Rat, G. Pantel, S. Wilker, Heat Flow Calorimetry of Propellants - Effects of Sample Preparation and Measuring Conditions, *Propellants Explos. Pyrotech.* **2001**, *26*, 51–57, DOI:10.1002/1521-4087(200104)26:2<51::AID-PREP51>3.0.CO;2-H.

[8] M. Heil, J. Hickmann, C. Müller, Thermal Characterization of Naturally Aged Propellants, *Propellants Explos. Pyrotech.* **2019**, *44*, 687–695, DOI:10.1002/prep.201800334.

[9] N. Halilovic, M. Kaucic-Skufca, Z. Ademovic, A. Basic-Halilovic, R. Omanovic, Analysis of Stability of Naturally Aged Single Base Propellants, *African J. Pure Appl. Chem.* **2021**, *15*, 1–7, DOI:10.5897/ajpac2020.0859.

[10] D. Setyaningsih, A. L. Juwono, H. Supriyatno, Stabilizer Effect on Thermal Decomposition of Aged Solid Propellant, *J. Phys. Conf. Ser.* **2017**, *909*, DOI:10.1088/1742-6596/909/1/012077.

[11] A. Chin, D. S. Ellison, S. K. Poehlein, M. K. Ahn, Investigation of the Decomposition Mechanism and Thermal Stability of Nitrocellulose/Nitroglycerine Based Propellants by Electron Spin Resonance, *Propellants Explos. Pyrotech.* **2007**, *32*, 117–126, DOI:10.1002/prep.200700013.

[12] D. Trache, A. F. Tarchoun, Stabilizers for Nitrate Ester-Based Energetic Materials and Their Mechanism of Action: A State-of-the-Art Review, Springer US, *J. Mater. Sci.* **2018**, *53*, 100–123, DOI:10.1007/s10853-017-1474-y.

[13] C. P. Lin, J. S. Li, J. M. Tseng, M. S. Mannan, Thermal Runaway Reaction for Highly Exothermic Material in Safe Storage Temperature, Elsevier Ltd, *J. Loss Prev. Process Ind.* **2016**, *40*, 259–265, DOI:10.1016/j.jlp.2016.01.006.

[14] P. Krumlinde, S. Ek, E. Tunestal, A. Hafstrand, Synthesis and Characterization of Novel Stabilizers for Nitrocellulose-Based Propellants, *Propellants Explos. Pyrotech.* **2017**, *42*, 78–83, DOI:10.1002/prep.201600122.

[15] L. S. Lussier, E. Bergeron, H. Gagnon, Study of the Daughter Products of Akardite-II, *Propellants Explos. Pyrotech.* **2006**, *31*, 253–262, DOI:10.1002/prep.200600034.

[16] O. Frys, P. Bajerova, A. Eisner, J. Skladal, K. Ventura, Utilization of New Non-Toxic Substances as Stabilizers for Nitrocellulose-Based Propellants, *Propellants Explos. Pyrotech.* **2011**, *36*, 347–355, DOI:10.1002/prep.201000043.

[17] S. Wilker, G. Heeb, B. Vogelsanger, J. Petrzílek, J. Skladal, Triphenylamine - A "new" Stabilizer for Nitrocellulose Based Propellants - Part I: Chemical Stability Studies, *Propellants Explos. Pyrotech.* **2007**, *32*, 135–148, DOI:10.1002/prep.200700014.

[18] J. Bladek, S. Wilker, S. Pietrzyk, S. Cudzilo, A Novel Method for Testing Propellant Stabilizers, *Cent. Eur. J. Energ. Mater.* **2010**, *7*, 281–287.

[19] M. A. Zayed, A. A. W. Soliman, M. A. Hassan, Evaluation of Malonanilides as New Stabilizers for Double-Base Propellants. (I),

J. Hazard. Mater. **2000**, *73*, 237–244, DOI:10.1016/S0304-3894(99)00153–3.

[20] M. A. Zayed, A. A. Mohamed, M. A. M. Hassan, Stability Studies of Double-Base Propellants with Centralite and Malonanilide Stabilizers Using MO Calculations in Comparison to Thermal Studies, Elsevier B. V., *J. Hazard. Mater.* **2010**, *179*, 453–461, DOI:10.1016/j.jhazmat.2010.03.025.

[21] M. A. Hassan, Effect of Malonyl Malonanilide Dimers on the Thermal Stability of Nitrocellulose, *J. Hazard. Mater.* **2001**, *88*, 33–49, DOI:10.1016/S0304-3894(01)00297–7.

[22] Q. Tang, X. Fan, J. Li, F. Bi, X. Fu, L. Zhai, Experimental and Theoretical Studies on Stability of New Stabilizers for N-Methyl-P-Nitroaniline Derivative in CMDB Propellants, Elsevier B. V., *J. Hazard. Mater.* **2017**, *327*, 187–196, DOI:10.1016/j.jhazmat.2016.12.049.

[23] G. Li, B. Jin, Z. Chai, L. Liao, S. Chu, R. Peng, Synthesis and Stabilization Mechanism of Novel Stabilizers for Fullerene-Malonamide Derivatives in Nitrocellulose-Based Propellants, Elsevier Ltd, *Polym. Test.* **2020**, *86*, 106493, DOI:10.1016/j.polymertesting.2020.106493.

[24] E. Tunestål, A. Hafstrand, A. Lindborg, S. Ek, P. Goede, P. Krumlinde, C. Schragen, New stabilizers for NC-propellants Evaluated in Rocket Propellants, *Insensitive Munitions Energ. Mater. Technol. Symp.*, Rome, Italy, May 18–21 **2015**, https://imemg.org/wp-content/uploads/2015/06/2 A2-17467-New-stabilizers-for-NC-propellants-final.pdf.

[25] M. A. Zayed, S. E. M. El-Begawy, H. E. S. Hassan, Mechanism Study of Stabilization of Double-Base Propellants by Using Zeolite Stabilizers (Nano- and Micro-Clinoptilolite), King Saud University, *Arab. J. Chem.* **2017**, *10*, 573–581, DOI:10.1016/j.arabjc.2013.08.021.

[26] A. Dejeaifve, A. Sarbach, B. Roduit, P. Folly, R. Dobson, Making Progress Towards «Green» Propellants – Part II, *Propellants Explos. Pyrotech.* **2020**, *45*, 1185–1193, DOI:10.1002/prep.202000059.

[27] R. L. B. Rodrigues, M. F. Lemos, T. C. C. França, L. G. M. Filho, Development of Nitrocellulose-Based Propellants with Natural Stabilizers, *J. Aerosp. Technol. Manag.* **2019**, *11*, 3–6, DOI:10.5028/jatm.etmq.40.

[28] R. L. B. Rodrigues, P. A. Gomes Buitrago, N. L. Nakano, F. C. Peixoto, M. F. Lemos, T. C. C. França, L. G. Mendonça Filho, Can Green Nitrocellulose-Based Propellants Be Made through the Replacement of Diphenylamine by the Natural Product Curcumin?, Taylor & Francis, *J. Energ. Mater.* **2021**, *00*, 1–24, DOI:10.1080/07370652.2020.1859646.

[29] A. Dejeaifve, R. Dobson, Ionone Stabilisers for Nitrocellulose-Based Propellants, **2018**, US 2018/0029951 A1, PB Clermont, Engis, Belgium.

[30] K. Ganczyk-Specjalska, Conventional and Alternative Nitrocellulose Stabilisers Used in Gun Propellants, High Energy Materials, *Conv. Altern. Nitrocellul. stabilisers used gun propellants* **2019**, 73–82, DOI:10.22211/matwys/0175.

[31] J. A. Mathis, B. R. McCord, Gradient Reversed-Phase Liquid Chromatographic-Electrospray Ionization Mass Spectrometric Method for the Comparison of Smokeless Powders, *J. Chromatogr. A* **2003**, *988*, 107–116, DOI:10.1016/S0021-9673(02)-02055–1.

[32] K. L. Reese, A. D. Jones, R. W. Smith, Characterization of Smokeless Powders Using Multiplexed Collision-Induced Dissociation Mass Spectrometry and Chemometric Procedures, Elsevier Ireland Ltd, *Forensic Sci. Int.* **2017**, *272*, 16–27, DOI:10.1016/j.forsciint.2016.12.021.

[33] M. Lopez-Lopez, A. F. de la O. Maria, S. G. Jorge, L. F. Jose, V. Alfonso, T. Mercedes, G.-R. Carmen, New Protocol for the Isolation of Nitrocellulose from Gunpowders: Utility in Their Identification, *Talanta* **2010**, *81*, 1742–1749, DOI:10.1016/j.talanta.2010.03.033.

[34] A. M. Walwil, The Mass Spectra Analysis for α-Ionone and β-Ionone, *Int. J. Chem.* **2017**, *9*, 61, DOI:10.5539/ijc.v9n3p61.

[35] E. D. Babot, C. Aranda, J. C. Del RÍo, R. Ullrich, J. Kiebist, K. Scheibner, M. Hofrichter, A. T. MartÍnez, A. Gutiérrez, Selective Oxygenation of Ionones and Damascones by Fungal Peroxygenases, *J. Agric. Food Chem.* **2020**, *68*, 5375–5383, DOI:10.1021/acs.jafc.0c01019.

[36] M. Szori, C. Fittschen, I. G. Csizmadia, B. Viskolcz, Allylic H-Abstraction Mechanism: The Potential Energy Surface of the Reaction of Propene with OH Radical, *J. Chem. Theory Comput.* **2006**, *2*, 1575–1586, DOI:10.1021/ct600140b.

[37] J. Hoggett, R. B. Moodie, J. R. Penton, K. Schofield, Nitration and Aromatic Reactivity., Syndics Of The Cambridge University Press, *Cambridge Univ. Press* **1972**, *84*.

[38] G. Wypych, Uv Degradation & Stabilization of Polymers & Rubbers, *Handb. UV Degrad. Stab.* **2015**, DOI:10.1016/b978-1-895198-86-7.50009–7.

[39] R. Radi, Nitric Oxide, Oxidants, and Protein Tyrosine Nitration, *Proc. Natl. Acad. Sci. USA* **2004**, *101*, 4003–4008, DOI:10.1073/pnas.0307446101.

Manuscript received: June 25, 2021
Revised manuscript received: August 16, 2021
Version of record online: September 24, 2021